

See discussions, stats, and author profiles for this publication at: <https://www.researchgate.net/publication/7162386>

Phosphorylation of a Single Head of Smooth Muscle Myosin Activates the Whole Molecule †

ARTICLE *in* BIOCHEMISTRY · MAY 2006

Impact Factor: 3.02 · DOI: 10.1021/bi060154c · Source: PubMed

CITATIONS

12

READS

15

3 AUTHORS, INCLUDING:



Art Rovner

Haematologic Technologies Inc.

24 PUBLICATIONS 933 CITATIONS

SEE PROFILE

Published in final edited form as:

Biochemistry. 2006 April 25; 45(16): 5280–5289.

Phosphorylation of a Single Head of Smooth Muscle Myosin Activates the Whole Molecule†

Arthur S. Rovner, Patricia M. Fagnant, and Kathleen M. Trybus*

Department of Molecular Physiology and Biophysics, Health Sciences Research Facility, University of Vermont, Burlington, VT 05405

Abstract

Regulatory light chain (RLC) phosphorylation activates smooth and non-muscle myosin IIs, but it has not been established if phosphorylation of one head turns on the whole molecule. Baculovirus expression and affinity chromatography were used to isolate heavy meromyosin (HMM) containing one phosphorylated and one dephosphorylated RLC (1-P HMM). Motility and steady-state ATPase assays indicated that 1-P HMM is nearly as active as HMM with two phosphorylated heads (2-P HMM). Single turnover experiments further showed that both the dephosphorylated and phosphorylated heads of 1-P HMM can be activated by actin. Singly-phosphorylated full-length myosin was also an active species with two cycling heads. Our results suggest that phosphorylation

†This work was supported by NIH Grants AR47906 and HL38113 to KMT

*To whom correspondence should be addressed: Department of Molecular Physiology and Biophysics, 130 Health Sciences Research Facility, University of Vermont, Burlington, VT 05405-0068. Phone: (802) 656-8750. Fax: (802) 656-0747. E-mail: kathleen.trybus@uvm.edu

¹Abbreviations:

RLC	regulatory light chain
HMM	heavy meromyosin, the soluble, two-headed fragment of myosin
1-P HMM	expressed heavy meromyosin with one phosphorylated head
2-P HMM	expressed heavy meromyosin with two phosphorylated heads
AA-RLC	smooth muscle myosin regulatory light chain with alanine residues substituted for Thr18 and Ser19
1-P myosin	myosin with one phosphorylated head
0-P myosin	exchanged myosin with two HIS-tagged AA-RLCs
mant-dATP	3'-O-(N-methyl-anthraniloyl)-2'-deoxy-adenosine 5'-triphosphate, 2-P myosin, myosin with two phosphorylated heads
deP myosin	dephosphorylated myosin
deP HMM	expressed, dephosphorylated heavy meromyosin
S1	subfragment 1, a single-headed fragment of myosin

of one RLC abolishes the asymmetric inhibited state formed by dephosphorylated myosin, allowing activation of both the phosphorylated and dephosphorylated heads. These findings help explain how smooth muscles are able to generate high levels of stress with low phosphorylation levels.

The activity of smooth and non-muscle myosin II is regulated by phosphorylation of the RLC (reviewed in (1)). Phosphorylation accelerates the release of inorganic phosphate by several hundred-fold (2). The critical RLC sequences involved in this regulation were defined by exchange of expressed mutant light chains into myosin (3-5). Additional insights came from studies which showed that only double-headed molecules could achieve the fully inhibited state, whereas single heads of myosin or constructs with one intact and one truncated head were active without phosphorylation (6-9). A minimal length of the coiled-coil rod region of the tail was required for full phosphorylation-dependent regulation of the molecule, as well as flexibility in the first two heptads of the coiled-coil at the junction between the two heads (10). These observations indicated that maintenance of the inactive state involves the interaction of the two heads with each other and/or with the rod, and that phosphorylation alters or abolishes these interactions.

A major breakthrough in understanding the mechanism of regulation came from 3D image reconstruction of dephosphorylated and phosphorylated HMM and myosin (11). The dephosphorylated species showed an asymmetric interaction between the two heads of a molecule, with the actin-binding region of one head bound to the converter region of the second head (11,12). One head cannot bind to actin, and the second head cannot rotate its converter region, which is necessary for progression through the ATPase cycle. The conformation adopted by dephosphorylated myosin thus prevents actin-activated ATPase activity by either head, but by different mechanisms. Conversely, in phosphorylated HMM or myosin, the head-head interaction is abolished, allowing both heads to bind actin and proceed through their enzymatic cycles. These structural data highlighted the features of the inhibited state and provided an explanation for many of the earlier biochemical and mutational studies.

An important question which has attracted considerable interest is whether myosin which has been phosphorylated on only one head has activity comparable to that of doubly-phosphorylated myosin. Data from physiological studies show that smooth muscle tissues which are generating near-maximal levels of tension in many cases have very low levels of RLC phosphorylation (13-15). Phosphorylation of the two heads of myosin is random (16, 17), and thus there will be a large proportion of singly-phosphorylated molecules at low levels of phosphorylation, which need to be active to account for the physiologic data. Nonetheless, data from biochemical studies have failed to support this idea, suggesting either that both crossbridge heads must be phosphorylated to significantly activate the molecule (negative cooperativity; (18-20)), or that phosphorylation independently activates each head (21,22). A complicating factor in these studies was that conclusions were drawn by assaying a heterogeneous mixture of dephosphorylated, singly- and doubly-phosphorylated molecules. Only one study succeeded in isolating the singly-phosphorylated molecule in pure form, but the large discrepancies between steady-state and single-turnover measurements complicated the interpretation of the data. The authors concluded that the singly-phosphorylated species was far less active (7-19%) than the doubly-phosphorylated species (23).

Here we used the baculovirus/insect cell expression system to isolate homogeneous preparations of smooth muscle HMM with only one phosphorylated head, by employing a differential tagging strategy and affinity chromatography (24). Motility, actin-activated ATPase, and single turnover assays indicated that both 1-P HMM and 1-P myosin are active species. Our results suggest that phosphorylation of a single head is sufficient to liberate both heads of the molecule from the inhibited asymmetric conformation described above, thus allowing either the phosphorylated or the dephosphorylated head to be activated by actin. These

data provide a mechanistic explanation for how smooth muscles can develop high levels of force with minimal levels of myosin phosphorylation.

EXPERIMENTAL PROCEDURES

Production of Recombinant Baculoviruses

Thr18 and Ser19 of the wild-type chicken gizzard RLC cDNA (4) were mutated to Ala, and a FLAG tag (DYKDDDDK) was added to the N-terminus (AA-RLC). A hexa-histidine tag (HIS) was added to the N-terminus of the wild-type RLC cDNA (WT-RLC). Both RLCs had a thrombin recognition site after the tag which upon proteolysis added a single N-terminal Gly residue to the RLC sequence. The N-terminal sequences of the two light chains preceding the coding sequence were (HIS)₆-VLVPRG or DYKDDDDK-VLVPRG. Initially, the two RLC cDNAs were cloned into the vector pACSG2 (24) and created as separate baculoviruses. Later work utilized a double RLC viral construct modified from the transfer vector pAcDB3 (BD-Pharmingen), with one polyhedrin promoter and two p10 promoters.

The cDNA for the chicken gizzard myosin heavy chain cDNA (25) was truncated after glutamic acid 1,175 to encode HMM, and cloned into the transfer vector pVL1393, which had been modified to include an Nco I site at the initiation codon (26). A C-terminally FLAG-tagged subfragment-1 (S1) containing both the essential and regulatory light chains was also synthesized.

Infection of Sf9 Cells and 1-P HMM Purification

Smooth muscle HMM containing one HIS-tagged WT-RLC and one FLAG-tagged AA-RLC was produced by co-infecting Sf9 insect cells with four viruses; one for each of the two RLC types, one for the smooth muscle myosin essential light chain, and one encoding the 1,175 amino acid HMM heavy chain. Later experiments utilized a virus expressing both forms of the RLC, allowing more equal expression of the two RLCs.

Cells were lysed, ammonium sulfate fractionated, and dialyzed overnight with a slight molar excess of actin (24). The acto-HMM was pelleted, leaving excess RLCs in the supernatant. The pellet was washed with a buffer containing 0.1 M NaCl, 10 mM imidazole (pH 7.4, 4°C); 1 mM ethylene glycol-bis(2-aminoethylether)-N,N,N',N'-tetraacetic acid (EGTA); 1 mM dithiothreitol (DTT), 7% (w/v) sucrose, and 5 µg/ml leupeptin, and re-centrifuged. The pellet was suspended in the same buffer and HMM was eluted by adding 1.5 mM MgATP (3-4 times) followed by centrifugation.

1-P HMM was isolated in homogeneous form by successive chromatographic purification steps, as illustrated by SDS and charge-sensitive gels (Fig. 1A, B). The HIS and FLAG tags imparted unique mobility to the WT-RLC and AA-RLCs, so that they could be distinguished in the actin-eluted material loaded onto an anti-FLAG M2 column (Sigma Chemical) (27) (Fig. 1A, lane 1). Western blots with FLAG- and HIS-specific antibodies confirmed the identity of the two RLCs (data not shown). The RLC which flowed through the FLAG column was almost exclusively HIS-tagged (Fig. 1A, lane 2). Bound protein eluted by competition with FLAG peptide contained predominantly the FLAG-tagged RLC, consistent with the presence of homodimers (two FLAG-tagged RLCs) and heterodimers (one HIS-tagged and one FLAG-tagged RLC) (Fig. 1A, lane 3).

The concentration of NaCl was increased to 0.3 M before loading the FLAG eluate onto a nickel-chelate column (HisTrap 5 ml; Amersham Biosciences), on an FPLC system (AktaFPLC - GE Healthcare). The column was washed with 0.3 M NaCl, 10 mM (3-(N-Morpholino)-propanesulfonic acid) (MOPS) (pH 7.5, 4°C), 1 mM EGTA, and 0.5 mM DTT, then washed with the same buffer containing 15 mM imidazole to remove non-specifically

bound FLAG-tagged AA-RLC homodimers (Fig. 1A, lane 4). Heterodimeric HMMs (one FLAG-tagged AA-RLC and one HIS-tagged WT-RLC) were eluted using the above buffer containing 0.3 M imidazole (Fig. 1A, lane 5). The heterodimer pool showed two RLC bands on a gel system which is sensitive to changes in charge (Fig. 1B, lane 3).

The N-terminal epitope tags were removed by thrombin (Haematologic Technologies; 1 unit/mg protein) while dialyzing overnight in a buffer containing 50 mM NaCl, 10 mM (N-[2-Hydroxyethyl]piperazine-N'-[2-ethanesulfonic acid]) (Hepes) (pH 7.2, 4°C), 1 mM EGTA, and 1 mM DTT. After this treatment, the AA-RLCs and WT-RLCs co-migrated as a single band, while the HMM heavy chains were unaffected (Fig. 1A, lane 6; Fig. 1B, lane 4). The next day, protease inhibitors were added to permanently inhibit the thrombin (0.5 mM 4-(2-aminoethyl)-benzenesulfonyl fluoride hydrochloride (AEBSF), 0.5 mM N α -p-Tosyl-L-lysine chloromethyl ketone hydrochloride (TLCK), and 10 μ g/ml leupeptin).

Myosin light chain kinase (3-4 μ g/ml) was used with Ca²⁺ (0.5 mM), calmodulin (7.5 μ g/ml) and MgATP γ S (1.5 mM) to thiophosphorylate the WT-RLCs, causing a shift in their mobility on charge-sensitive gels to the same position as the control phosphorylated RLC (Fig. 1B, compare lane 5 with lane 2). The presence of comparable amounts of two RLCs with the mobilities of control dephosphorylated and phosphorylated RLC supports our contention that the purified HMM is a homogeneous population of molecules with one thiophosphorylated head (WT-RLC) and one dephosphorylated head (AA-RLC). For storage at -20°C, 1-P HMM was dialyzed into a buffer containing 50 mM NaCl, 10 mM imidazole (pH 7.4, 4°C), 1 mM EGTA, 3 mM NaN₃, 1.5 mM DTT, and 50% glycerol

HMM with two WT-RLCs or S1 was expressed and purified from the baculovirus system using a FLAG tag located at the C-terminus of the heavy chain (27). The homogeneity of the expressed HMM preparation was evaluated by chromatography on a monoQ column (Akta FPLC system, G.E. Healthcare). A gradient of NaCl from 10 mM to 500 mM NaCl was used in a base buffer containing 10 mM imidazole (pH 7.4, 22°C), 1 mM EGTA, 0.5 mM DTT. The HMM eluted in a single symmetrical peak at about 370 mM NaCl. Analysis of this species by single turnovers showed no difference from expressed HMM which was not chromatographed.

Purification of Chicken Gizzard Myosin and Bacterially-Expressed AA-RLCs

Myosin was prepared from chicken gizzards (27) with the modification that the first ammonium sulfate fractionation went to 37% saturation. The mutant AA-RLC cDNA was cloned into the expression vector pT7-7 with an N-terminal HIS tag followed by a thrombin cleavage site (N-terminal sequence preceding the coding region is (HIS)₆-AM-VLVPRG). After expression in *E. coli*, the light chain was isolated from washed inclusion bodies (4), and purified on an anion exchange column (DEAE Sephacel; GE Healthcare), with a gradient from 5 to 400 mM NaCl. Pooled fractions were dialyzed versus 50 mM NaCl, 5 mM Na-PO₄ (pH 7.2, 4°C), and lyophilized.

Light Chain Exchange and Purification of Singly-Phosphorylated Myosin (1-P Myosin)

Thiophosphorylated myosin (1.0 mg/ml) was incubated with a 3-fold molar excess of HIS-tagged AA-RLCs (0.24 mg/ml) in a buffer containing 0.6 M KCl, 10 mM K-PO₄ (pH 7.5), 1 mM EGTA, 10 mM ethylenediaminetetraacetic acid (EDTA), 2 mM ATP, and 5 mM DTT for 30 min at 37°C, allowing ~50% exchange of mutant RLCs into the myosin. The reaction was cooled and MgCl₂ was added to 15 mM. Following dialysis versus a low salt buffer (40 mM NaCl, 10 mM imidazole-hydrochloride (pH 7.0, 4°C), 10 mM MgCl₂, 1 mM EGTA, 1 mM DTT), the precipitated myosin was collected by centrifugation, washed in the same buffer, and sedimented. The pellet was dissolved in a minimal volume of buffer A (0.5 M NaCl, 20 mM Na-PO₄ (pH 7.5, 4°C)) plus 1 mM DTT, and dialyzed overnight against buffer A. The exchange

procedure yielded homodimers with two phosphorylated native RLCs, heterodimers with one HIS-tagged AA-RLC and one phosphorylated native RLC, and homodimers with two HIS-tagged AA-RLCs. The RLC species were identified on SDS gels by their differing mobilities (Fig. 2).

A HiTrap 5 ml. chelating column (GE Healthcare) equilibrated with Buffer A on the AktaFPLC system was used to separate HIS-tagged and untagged species. The exchanged myosin contained nearly equal amounts of the HIS-tagged and phosphorylated native RLC (Fig. 2, lane 1). Washing the column with buffer A containing 15 mM imidazole displaced non-specifically bound myosin with two phosphorylated native RLCs as well as a small amount of AA-RLC (Fig. 2, lane 2). The column was eluted with a gradient of imidazole from 15 to 300 mM in buffer A (25 column volumes), displacing first singly HIS-tagged, 1-P myosin molecules (Fig. 2, lane 3), then doubly-tagged molecules with two AA-RLCs later in the gradient (0-P myosin) (Fig. 2, lane 5).

To remove the N-terminal HIS tag, 1 mM EGTA, 0.5 mM DTT, and thrombin (1 Unit/mg protein) were added to 1-P myosin. After 4-6 hours dialysis versus 25 mM NaCl, 10 mM Hepes (pH 7.35, 4°C), 1 mM EGTA, 0.5 mM DTT, proteolysis was terminated by adding 0.5 mM AEBSF, 0.5 mM TLCK, and 10 µg/ml leupeptin. Removal of the HIS tag caused the recombinant AA-RLC to comigrate with the native RLC on the SDS gel (Fig. 2, lanes 4, 6).

1-P myosin was polymerized by addition of 20 mM MgCl₂, and by lowering the pH to 6.8. The precipitated material was collected by centrifugation, and the pellet was washed and sedimented in dialysis buffer with the above protease inhibitors plus 10 mM MgCl₂. The singly-exchanged, 1-P myosin was dissolved in and dialyzed versus Buffer A with 1 mM EGTA, 1.5 mM DTT, 0.5 mM AEBSF, 10 µg/ml leupeptin, and 50% glycerol for storage at -20°C.

Thiophosphorylation of Smooth Muscle HMM and Myosin

Myosin was phosphorylated in the filamentous state using endogenous Ca²⁺-sensitive kinase activity, adding CaCl₂, calmodulin, and MgATPγS to concentrations of 0.5 mM free, 7.5 µg/ml, and 1.5 mM, respectively. The buffer contained 20 mM NaCl, 10 mM Na-PO₄ (pH 7.5, 4°C), 5 mM MgCl₂, 1 mM EGTA, 1 mM DTT.

Gels

Pre-cast 12% SDS-acrylamide gels (Bio-Rad) were used to follow the protein purification procedure. A glycerol-containing charge separation gel system was used to determine the level of RLC phosphorylation (27).

Motility and Steady-State ATPase Assays

Actin filament motility was measured as described (24,27) in a 25 mM KCl buffer. Antibody S2.2 was used to attach the HMMs to the motility surface. Steady-state actin-activated ATPase assays were conducted at 37°C in 10 mM imidazole (pH 7.0), 1 mM MgCl₂, 1 mM EGTA, 1 mM NaN₃, and 1 mM DTT, along with 10 mM NaCl for HMM and 60 mM NaCl for myosin (24,27). Myosin was also assayed in a buffer with 10 mM MgCl₂ to minimize formation of the folded 10S conformation. Smooth muscle tropomyosin was added to myosin assays at a molar ratio to actin of 1:6. The maximum activity (V_{max}), and the actin concentration at half-maximal activity (K_M) were derived from fitting the data to the Michaelis-Menten equation.

Single Turnover ATPase Assays

HMM and myosin were dialyzed to remove all nucleotide that had been used for phosphorylation. The buffer was the same as that used for steady-state ATPase assays (above),

and the temperature was 30°. Single turnovers with HMM were done using a Kin-Tek SF-2002 stopped-flow spectrophotometer.

The first single turnover technique employed fluorescent 3'-O-(N-methyl-anthraniloyl)-2'-deoxy-adenosine 5'-triphosphate (mant-dATP) (Jena Biosciences) in a double-mixing protocol, with excitation at 360 nm (4 nm band width), and emission monitored with a 400 nm cutoff filter. 1.5 μ M HMM was rapidly mixed with 3 μ M mant-dATP and the mixture was incubated 1.5 seconds to allow mant-dATP binding to HMM. This complex was then mixed with varying concentrations of actin and 3 mM MgATP. Fluorescence decreased as mant-dADP was released and subsequently replaced by MgATP. The final, post-mixing concentrations of the reagents used in this reaction were 0.5 μ M HMM, 1.0 μ M mant-dATP, 1.0 mM MgATP, and 2.5, 5, or 10 μ M actin.

In the second single-mixing stop-flow protocol, HMM, varying concentrations of actin, and hexokinase in syringe 1 were mixed with MgATP and glucose in syringe 2 (28). Excitation was at 295 nm (10 nm band width), and emission monitored using a 295 nm interference filter. Following mixing, the signal rapidly decreased as actoHMM was dissociated by ATP. Excess MgATP was hydrolyzed by the hexokinase/glucose system, limiting each HMM molecule to a single turnover, and light scattering then increased as HMM reassociated with actin. The concentrations of the reagents following mixing were 0.5 μ M HMM, actin (2.5, 5, and 10 μ M), 25 Units/ml hexokinase, 50 μ M MgATP, and 2 mM glucose. Controls were performed to verify that single turnovers were taking place. There was no change in rate if the final concentration of hexokinase was halved (12.5 Units/ml) or doubled (50 Units/ml). The ATP concentration was varied both in the presence (25 Units/ml of hexokinase) or absence of the glucose/hexokinase system. ATP concentrations from 50 to 200 μ M showed complete acto-HMM dissociation, but no delay upon reassociation with actin. HMM data traces were fitted to either single or double exponential equations using Kintek software (version 8.1.0). The validity of double exponential fits was confirmed by comparing the residuals from these plots with those from single exponential fits.

Single turnover experiments for myosin were conducted using mant-dATP in the absence of actin. Due to the long time courses, these measurements were conducted with a steady-state K2 fluorimeter (ISS), which allowed periodic shuttering of the exciting light. The buffer was 100 mM NaCl, 10 mM imidazole-hydrochloride (pH 7.0, 37°C), 1 mM EGTA, 1 mM NaN₃, 5 mM MgCl₂, and 1 mM DTT. Myosin was added to a cuvette containing mant-dATP, and after fluorescence values reached their maximum, unlabeled MgATP was added. The final concentration of reagents after mixing was the same as mant-dATP single turnovers with HMM. Data were collected every 6 or 15 sec for 1 sec, shuttering the exciting light between time points to prevent photobleaching. The experiment was continued until fluorescence reached values similar to those before the addition of protein to the cuvette.

Single turnover time courses were normalized to a full-scale signal change of 1.0 by subtracting the minimum from all other values in the time course, and then dividing by the maximum signal value. For experiments with myosin, these normalized traces were fit to exponential equations using Slidewrite software (Advanced Graphics Software).

Analytical Ultracentrifugation

Myosins (2-P, 1-P, and deP) were dialyzed into 0.6 M KCl, 10 mM K-PO₄ (pH 7.4, 4°C), 1 mM EGTA, 1 mM NaN₃, and 1 mM DTT. The proteins were clarified and then dialyzed versus 0.15 M KCl, 10 mM K-PO₄ (pH 7.4, 4°C), 5 mM MgCl₂, 1 mM EGTA, 1 mM NaN₃, and 1 mM DTT. MgATP was added to 0.25 mM, and the protein samples were analyzed in a Beckman Optima XL-I analytical ultracentrifuge at 20,000 and 50,000 rpm (20°C). The low-speed spin established the percent filaments, while the sedimentation coefficient of the soluble material

was obtained from data at the higher speed. The program DCDT+ was used to derive the apparent sedimentation coefficient distribution function $g(s^*)$ versus s^* from the sedimentation data (29).

RESULTS

Purification of 1-P HMM

A smooth muscle HMM that can be phosphorylated on only one of its two heads was prepared by expressing heterodimeric HMM molecules in the baculovirus system. The heterodimers contain both a HIS-tagged WT RLC, and a FLAG-tagged non-phosphorylatable AA-RLC (T18A/S19A). This dual epitope-tagging strategy (24) allowed us to completely separate these molecules from the corresponding homodimers in Sf9 cell lysates using sequential affinity chromatography on FLAG and nickel-chelate columns, as described in detail in Methods (see Fig. 1). The epitope tags were removed from both RLC sequences by thrombin cleavage prior to functional analysis of the HMM. The presence of a non-phosphorylatable light chain on one head of this molecule allowed us to thiophosphorylate the final purified protein with no possibility of contamination by the active doubly phosphorylated species.

Motility and Actin-activated ATPase Activity of HMMs

The actin filament sliding velocity supported by 1-P HMM was nearly 90% that of 2-P HMM (0.88 ± 0.14 $\mu\text{m}/\text{sec}$ versus 1.02 ± 0.11 $\mu\text{m}/\text{sec}$) (Fig. 3A). The quality of the movement was very similar for the two types of HMM, with all of the filaments moving smoothly for most preparations. Dephosphorylated HMM (deP HMM) did not support actin motility.

The maximum steady-state actin-activated ATPase for 1-P HMM was 3.1 ± 0.4 sec^{-1} versus 4.8 ± 0.6 sec^{-1} for 2-P HMM, while the K_M values were similar (26 ± 9 μM versus 32 ± 10 μM) (Fig. 3B). The activity of deP HMM was much lower than the other two species. Thus, under steady-state conditions, 1-P HMM has more than half the activity of 2-P HMM.

Single-Turnover Analysis of HMMs by Mant-dATP Fluorescence

Steady-state ATPase assays give the average activity of the whole population over multiple turnovers, but cannot reveal the kinetic properties of the individual heads. To determine whether the two heads of 1-P HMM have different ATPase rates, we performed single turnover assays, in which each active site is allowed to hydrolyze only one molecule of ATP (see Methods). The first type of assay used a double mixing technique. The HMM species was mixed with the pure 3' isomer of fluorescent mant-dATP, aged to allow formation of ADP.P_i, and then mixed with varying concentrations of actin and an excess of unlabeled ATP. This technique allowed us to separately assess the individual kinetics of each head. The raw data for each protein preparation were alternatively fit with single and double exponential equations, and the residuals from these were compared (Fig. 4). This analysis showed that 1-P HMM was better fit by a double than a single exponential equation, indicating that it contained two populations of heads with different ATPase rates (Fig. 4B). 2-P HMM released fluorescent ADP at a somewhat faster rate than 1-P, but was also better fit by a double exponential (Fig. 4A). A plot of the faster measured rates for 1-P and 2-P HMM over a range of actin concentrations showed that the slope of the linear fit to the 1-P HMM data was approximately 65% of the slope for 2-P HMM (Fig. 5A). However, the slow rates were quite similar for 1-P and 2-P HMM and did not change significantly with actin concentration for either species (Fig. 5B, note the expanded y-axis). The amplitudes of the fast and slow signals were approximately equal, and did not vary with actin concentration, in most experiments for both types of HMM. These data suggested that, for both 1-P and 2-P HMMs, only one of the two heads is binding to actin and becoming activated, while the second head cycles at a slow, "basal" rate comparable to that of control 2-P HMM measured in the absence of actin (data not shown).

The slow rates for both HMM species were significantly faster than the single-exponential rate of deP HMM measured in separate experiments ($\sim .11 \text{ sec}^{-1}$ versus $.003 \text{ sec}^{-1}$; data not shown). This comparison implies that phosphorylation of one head can free both heads from the fully inhibited conformation that is unique to the dephosphorylated molecule.

As a control, we also measured the turnover of baculovirus-expressed S1 (Fig. 4C). This species was well fit by a single exponential equation, further strengthening the evidence that the double exponential fits for the two HMM species are a result of their double-headed structure. The ATPase rate of S1 increased with actin, but with a lesser slope than the fast rates for the double-headed species (Fig. 5A).

Single-Turnover Analysis of HMMs by Light Scattering

Additional single turnovers were performed by measuring light scattering of the acto-HMM complex. The positive features of this method are that it uses the native nucleotide ATP instead of an analog, and it is not subject to fluorescence photobleaching. However, the relative contributions of each head to the light scattering signal are less well understood. Control experiments in which the concentrations of hexokinase (used to remove ATP not bound to HMM) and ATP were varied established that each HMM head was binding and hydrolyzing only 1 molecule of ATP. As with the mant-dATP assay, light scattering demonstrated that both 1-P and 2-P HMMs were better fit by double than single exponential equations (Fig. 6A). When plotted as a function of actin, the fast rate for 1-P HMM increased and was approximately two-thirds of the fast rate for 2-P HMM (Fig. 6B). The slower rate constant was not sensitive to the concentration of actin for either species, and was five-eight-fold faster than the very slow single rate measured for deP HMM. The relative amplitudes of fast and slow signals were equal within experimental error at all actin concentrations assayed. These observations were very similar to those obtained from the mant-dATP single turnovers.

Isolation of Singly-Phosphorylated Smooth Muscle Myosin

Additional experiments were performed with tissue-purified chicken gizzard myosin to determine whether the results obtained with the expressed soluble HMM were applicable to the intact molecule, which is able to form filaments. Singly phosphorylated myosin was prepared by exchanging a HIS-tagged, non-phosphorylatable AA-RLC into thiophosphorylated myosin, and the different species from this reaction were separated on a nickel-chelate column. Unexchanged, 2-P myosin flowed through the column, and a gradient of imidazole was then used to separate singly-tagged, singly-phosphorylated 1-P myosin from doubly-tagged, non-phosphorylated 0-P myosin. The detailed purification protocol and accompanying gels that document homogeneity of this preparation are described in Methods (see Fig. 2). The HIS-tag was cleaved from the light chain prior to functional analysis.

Motility and Steady-State ATPase Activity of Myosin

We compared the motility of 1-P and 2-P myosin which originated from the same exchange reaction and purification procedure. The velocity of 1-P myosin was $0.60 \pm 0.10 \text{ } \mu\text{m/sec}$ versus $0.73 \pm 0.20 \text{ } \mu\text{m/sec}$ for 2-P myosin. 0-P myosin which contained two non-phosphorylatable AA-RLCs did not support actin movement (Fig. 7A). Thiophosphorylated myosin not subjected to exchange or the nickel-chelate column moved at $1.02 \pm 0.12 \text{ } \mu\text{m/sec}$.

The steady-state ATPase activity of the three species was measured in two buffers which differed in their MgCl_2 concentration (1 versus 10 mM). The higher magnesium concentration favors filament formation and minimizes the amount of folded 10S monomer which has very low activity (30), thus allowing us to compare all three species in a filamentous form. In 1 mM MgCl_2 , the V_{max} of 1-P myosin was $0.20 \pm 0.02 \text{ sec}^{-1}$ versus $0.50 \pm 0.2 \text{ sec}^{-1}$ for 2-P myosin, while the activity of deP myosin was negligible (Fig. 7B). At the higher MgCl_2 concentration,

the maximum activity of 1-P myosin increased to over 75% that of 2-P myosin (V_{\max} of $0.89 \pm 0.10 \text{ sec}^{-1}$ versus $1.15 \pm 0.04 \text{ sec}^{-1}$), while the K_M s for the two species remained similar (Fig. 7C). The activity of deP myosin was also elevated in this buffer.

Single Turnover Analysis

To avoid problems caused by the high viscosity of actin and myosin filaments, we assessed the single turnover rate of our myosin preparations using mant-ATP in the absence of actin. To measure these very slow rates, we used a shuttered fluorimeter, allowing data collection over much longer time courses without photobleaching (see Methods). 1-P myosin was better fit by a double than a single exponential equation, while both 2-P and deP myosin were well fit by single exponential equations (Fig. 8). The amplitudes of the fast and slow rates displayed by 1-P myosin were nearly equal, suggesting that they arise from the two heads on each molecule. The slower rate of 1-P myosin was three-fold faster than the rate for deP myosin. These results indicate that, as in HMM, phosphorylation of a single head is sufficient to activate the myosin molecule.

Conformational States of Myosin

At physiological ionic strength, smooth muscle myosin exists in equilibrium between filaments and a folded, inactive, monomeric species with a sedimentation coefficient of 10S. In the presence of MgATP, 2-P myosin preferentially assembles into filaments, while deP myosin is predominantly monomeric. Analytical ultracentrifugation (150 mM KCl and 0.25 mM MgATP) showed that 25-30% of the 1-P myosin sedimented as filaments, a value intermediate between that of 2-P myosin (75%) and deP myosin (10%). In all three samples the monomer which remained in equilibrium with polymer sedimented at 10S, indicating that 1-P myosin retains the ability to adopt the same folded monomeric conformation as do the fully phosphorylated and dephosphorylated species, although the propensity for formation of 10S versus filaments depends on phosphorylation levels.

DISCUSSION

Here we show that both singly-phosphorylated HMM and singly phosphorylated myosin are active species. They propel actin filaments at velocities nearly as fast as filaments moved by their doubly-phosphorylated counterparts. They display steady-state ATPase activities 65-75% as fast as the 2-P species. Single turnover analysis of 1-P HMM in the presence of actin further confirms that it has approximately two-thirds the activity of 2-P HMM, and that both heads are active. Dephosphorylation of both heads is therefore required for inhibition, but phosphorylation of one head is sufficient for activation.

Structural Model for Regulation of Smooth Muscle Myosin Activity

A recent structural model for regulation suggests that the heads of dephosphorylated smooth muscle myosin (or HMM) are inactive because they are locked in an asymmetric, intramolecular conformation (11,12) (see Fig. 9 cartoon, de-Phos). Despite some skepticism as to the validity of this mechanism for filaments *in vivo* (31), recent 3D reconstructions of striated thick filaments imaged by cryo-electron microscopy suggest that the two heads of dephosphorylated myosin also interact in a relaxed native filament (32). These interactions are disrupted upon phosphorylation of both heads, freeing them to interact with actin (33) (Fig. 9, 2-Phos).

Here, the striking similarity between our single turnover data for 1-P and 2-P HMM suggests that phosphorylation of one head is sufficient to disrupt the inhibited conformation, freeing both heads of 1-P HMM (Fig. 9, 1-Phos). The fast rate for both 1-P and 2-P HMM is dependent on actin concentration and thus reflects an actin-activated rate. Why is this rate approximately

two-thirds as fast for 1-P HMM as it is for 2-P HMM? First, we propose that it is equally likely that 1-P HMM binds to actin via a dephosphorylated head as via a phosphorylated head. Doubly phosphorylated HMM binds to actin with four-fold greater affinity than fully dephosphorylated HMM (34), but the structural model for regulation suggests that this is because only one head of dephosphorylated HMM is available to bind actin. Since there should be no such steric constraint on the heads of 1-P HMM, both dephosphorylated and phosphorylated heads should bind to and become actin-activated with equal frequency. Secondly, we suggest that a dephosphorylated head has somewhat lesser actin-activated ATPase activity than a phosphorylated head, and the rate for 1-P HMM reflects the average of approximately equal numbers of dephosphorylated and phosphorylated heads. Because heads with similar rates will not resolve into separate exponentials, this implies that the rate of a dephosphorylated head is similar to its phosphorylated counterpart.

The observation that a dephosphorylated head in a two-headed molecule can be active is not without precedent. In constructs where the rod region was truncated to 7-heptads or less of coiled-coil, but dimerization was enforced with a leucine zipper, dephosphorylated HMM molecules displayed a range of activities which were a sizeable percentage of the activity of doubly phosphorylated controls (10). Chimeric smooth muscle HMM constructs in which Loop 2 was replaced by skeletal myosin sequence moved actin filaments in the motility assay and had at least 50% of wild-type, phosphorylated ATPase activity, all in the absence of phosphorylation (35). These findings reinforce the idea that formation of the inhibited, intramolecular complex described above requires specific head/head and head/rod interactions, which can be disrupted in mutant or truncated constructs. Both here and in the previous work, the activity of dephosphorylated heads, while significant, was somewhat less than that of the equivalent phosphorylated construct. This lesser activity may be related to the lower affinity of the dephosphorylated RLC for its binding site in the neck region compared with a phosphorylated RLC, which could impact both on ATPase activity and the ability of the head to support force and movement. Consistent with this idea, a point mutation in a skeletal muscle myosin RLC that lowered its affinity for the heavy chain was shown to decrease the unitary step size and the rate of motility (36).

The single turnover assays also revealed a slower actin-independent rate for both 1-P and 2-P HMM, which we interpret as the intrinsic MgATPase activity of a head that is not bound to actin. The weak-binding conditions of the mant-dATP assay are likely to favor such single-headed interactions (Fig. 9). This suggestion is supported by laser trap studies on single-headed and heterodimeric molecules which indicated that one head performs all of the work on the actin filament (24,37,38). Single-headed binding is also consistent with the very low duty cycle which myosin II exhibits under unloaded conditions (4% for both smooth and skeletal in the motility assay) (39). An alternative explanation for the two rates is that they arise from two actin-bound heads of the same molecule. In this case, strain would be imposed on the heads, analogous to the situation proposed for the leading and trailing heads of myosin V (40). A restraining force would slow the ATPase kinetics relative to an unstrained head, and could be responsible for the slower rate that we observe.

Relationship to Previous Studies

A number of prior studies suggested that singly-phosphorylated myosin or HMM have low activity, but in only one case was this species purified to homogeneity before functional analysis (23). In this latter case, the investigators concluded that 1-P HMM had less than 20% the activity of 2-P HMM, despite steady state measurements suggesting that the former was at least half as active as the latter (23). These workers were unable to measure a rate comparable to 2-P HMM in single turnover measurements of 1-P HMM, and thus concluded that their relatively higher steady-state results were caused by a small, undetectable fraction of “rigor

heads". These differences from the present study are most likely because our HMM preparations were expressed using the baculovirus/insect cell expression system, thus ensuring an intact heavy chain, while the earlier study used proteolytically prepared HMM, which is cleaved at loop 2. The motility of 1-P HMM produced in the previous study was less than half that of the doubly phosphorylated control, while our expressed preparation was nearly 90% as fast as the control. Our single turnover assays showed two rates which in most cases had approximately equal signal amplitudes, consistent with each molecule having one fast and one slower head. No rate equivalent to that of a completely inhibited dephosphorylated head was observed, implying that an equilibrium between the fully active and inhibited states is unlikely. The agreement between our single turnover and steady state ATPase rates suggests that there was no sub-population of "rogue" molecules that dominate the steady-state assays.

Role of Singly-phosphorylated Myosin in the Latch State

Tonic smooth muscles such as those found in the vascular system are unique in that the relationships between Ca^{2+} concentration, RLC phosphorylation, tension development, and unloaded shortening velocity change during the course of contraction. Upon initial activation, these four parameters increase in concert. At maximal tension, RLC phosphorylation levels peak at 50-60%, and then gradually decrease to much lower levels, in parallel with decreasing Ca^{2+} and crossbridge cycling. During this time tension is maintained at its maximal level (reviewed in (41)). This dissociation between phosphorylation levels and the level of developed tension was termed "latch" (13).

The most plausible hypotheses to explain "latch" invoke a role for dephosphorylated heads in tension generation (reviewed in (42)). Hai and Murphy suggested that "latch bridges" are slowly-cycling myosin heads that are dephosphorylated after attachment to actin (43). The Somlyos and associates showed that in tonic smooth muscles, strain greatly slows the rate of ADP release and detachment from actin, particularly from dephosphorylated crossbridges (44,45). Butler and Siegman further postulated that a minimal level of "thiophosphorylation cooperatively activates the maximum number of myosin molecules, and a higher degree of thiophosphorylation makes the myosin cycle faster" (46). Although the isoform of myosin studied here is not typically expressed in smooth muscle tissues which exhibit latch, we believe that the mechanism by which singly phosphorylated molecules are activated which we describe is relevant to the latch phenomenon. Because phosphorylation is random (16,17), most of the activated molecules early in a contraction would be singly-phosphorylated, with an average cycling rate about two-thirds of maximum. As phosphorylation levels increase, these molecules will become doubly phosphorylated, with both heads cycling at the maximal rate. During the latch state, dephosphorylation would again produce a predominantly singly-phosphorylated population, in which dephosphorylated heads would play a prominent role in tension development. These heads will remain active until their partner head is dephosphorylated, and the fully inhibited state caused by intramolecular head interactions is obtained within the filament. Thus, it is likely that activation of dephosphorylated heads in singly-phosphorylated myosin molecules contributes to the formation of the latch state.

ACKNOWLEDGEMENTS

The authors thank Susan Lowey and all the members of the laboratory for critical reading of the manuscript, and Howard White for helpful comments.

REFERENCES

1. Sellers JR. Regulation of cytoplasmic and smooth muscle myosin. *Curr. Opin. Cell Biol* 1991;3(1): 98-104. [PubMed: 1854490]
2. Sellers JR. Mechanism of the phosphorylation-dependent regulation of smooth muscle heavy meromyosin. *J. Biol. Chem* 1985;260:15815-15819. [PubMed: 2933403]

3. Sweeney HL, Yang Z, Zhi G, Stull JT, Trybus KM. Charge replacement near the phosphorylatable serine of the myosin regulatory light chain mimics aspects of phosphorylation. *Proc. Natl. Acad. Sci. (USA)* 1994;91:1490–1494. [PubMed: 8108436]
4. Trybus KM, Chatman TA. Chimeric regulatory light chains as probes of smooth muscle myosin function. *J. Biol. Chem* 1993;268:4412–4419. [PubMed: 8440724]
5. Kamisoyama H, Araki Y, Ikebe M. Mutagenesis of the phosphorylation site (serine 19) of smooth muscle myosin regulatory light chain and its effects on the properties of myosin. *Biochemistry* 1994;33:840–847. [PubMed: 8292613]
6. Cremo CR, Sellers JR, Facemyer KC. Two heads are required for phosphorylation-dependent regulation of smooth muscle myosin. *J. Biol. Chem* 1995;270(5):2171–2175. [PubMed: 7836446]
7. Li XD, Saito J, Ikebe R, Mabuchi K, Ikebe M. The interaction between the regulatory light chain domains on two heads is critical for regulation of smooth muscle myosin. *Biochemistry* 2000;39:2254–2260. [PubMed: 10694391]
8. Konishi K, Kojima S, Katoh T, Yazawa M, Kato K, Fujiwara K, Onishi H. Two new modes of smooth muscle myosin regulation by the interaction between the two regulatory light chains, and by the S2 domain. *J. Biochem. (Tokyo)* 2001;129:365–372. [PubMed: 11226875]
9. Sweeney HL, Chen LQ, Trybus KM. Regulation of asymmetric smooth muscle myosin II molecules. *J Biol Chem* 2000;275:41273–41277. [PubMed: 11018047]
10. Trybus KM, Freyzon Y, Faust LZ, Sweeney HL. Spare the rod, spoil the regulation: necessity for a myosin rod. *Proc. Natl. Acad. Sci. U. S. A* 1997;94:48–52. [PubMed: 8990159]
11. Wendt T, Taylor D, Trybus KM, Taylor K. Three-dimensional image reconstruction of dephosphorylated smooth muscle heavy meromyosin reveals asymmetry in the interaction between myosin heads and placement of subfragment 2. *Proc. Natl. Acad. Sci. U. S. A* 2001;98:4361–4366. [PubMed: 11287639]
12. Liu J, Wendt T, Taylor D, Taylor K. Refined model of the 10S conformation of smooth muscle myosin by cryo-electron microscopy 3D image reconstruction. *J. Mol. Biol* 2003;329:963–972. [PubMed: 12798686]
13. Dillon PF, Aksoy MO, Driska SP, Murphy RA. Myosin phosphorylation and the cross-bridge cycle in arterial smooth muscle. *Science* 1981;211:495–497. [PubMed: 6893872]
14. Himpens B, Matthijs G, Somlyo AV, Butler TM, Somlyo AP. Cytoplasmic free calcium, myosin light chain phosphorylation, and force in phasic and tonic smooth muscle. *J. Gen. Physiol* 1988;92:713–729. [PubMed: 3216188]
15. Kamm KE, Stull JT. Myosin phosphorylation, force, and maximal shortening velocity in neurally stimulated tracheal smooth muscle. *Am. J. Physiol* 1985;249(18):C238–C247. [PubMed: 4037071]
16. Trybus KM, Lowey S. Mechanism of smooth muscle myosin phosphorylation. *J. Biol. Chem* 1985;260(29):15988–15995. [PubMed: 2933404]
17. Persechini A, Kamm KE, Stull JT. Different phosphorylated forms of myosin in contracting tracheal smooth muscle. *J. Biol. Chem* 1986;261(14):6293–6299. [PubMed: 3516992]
18. Persechini A, Hartshorne DJ. Phosphorylation of smooth muscle myosin: Evidence for cooperativity between the myosin heads. *Sci* 1981;213:1383–1385.
19. Ikebe M, Ogihara S, Tonomura Y. Nonlinear dependence of actin-activated Mg^{2+} -ATPase activity on the extent of phosphorylation of gizzard myosin and H-meromyosin. *J. Biochem. (Tokyo)* 1982;91:1809–1812. [PubMed: 6124540]
20. Sellers JR, Chock PB, Adelstein RS. The apparently negatively cooperative phosphorylation of smooth muscle myosin at low ionic strength is related to its filamentous state. *J. Biol. Chem* 1983;258(23):14181–14188. [PubMed: 6139378]
21. Chacko S. Effects of phosphorylation, calcium ion, and tropomyosin on actin-activated adenosine 5'-triphosphatase activity of mammalian smooth muscle myosin. *Biochemistry* 1981;20:702–707. [PubMed: 6452159]
22. Harris DE, Stromski CJ, Hayes E, Warshaw DM. Thiophosphorylation independently activates each head of smooth muscle myosin in vitro. *Am. J. Physiol* 1995;269:C1160–6. [PubMed: 7491905]
23. Ellison PA, Sellers JR, Cremo CR. Kinetics of smooth muscle heavy meromyosin with one thiophosphorylated head. *J Biol Chem* 2000;275:15142–15151. [PubMed: 10809750]

24. Rovner AS, Fagnant PM, Trybus KM. The two heads of smooth muscle myosin are enzymatically independent but mechanically interactive. *J. Biol. Chem* 2003;278:26938–26945. [PubMed: 12709440]
25. Yanagisawa M, Hamada Y, Katsuragawa Y, Imamura M, Mikawa T, Masaki T. Complete primary structure of vertebrate smooth muscle myosin heavy chain deduced from its complementary DNA Sequence. Implications on topography and function of myosin. *J. Mol. Biol* 1987;198:143–157. [PubMed: 2892941]
26. Trybus KM. Regulation of expressed truncated smooth muscle myosins. Role of the essential light chain and tail length. *J. Biol. Chem* 1994;269(33):20819–20822. [PubMed: 8063695]
27. Trybus KM. Biochemical studies of myosin. *Methods* 2000;22:327–335. [PubMed: 11133239]
28. Uyeda TQ, Tokuraku K, Kaseda K, Webb MR, Patterson B. Evidence for a novel, strongly bound acto-S1 complex carrying ADP and phosphate stabilized in the G680V mutant of Dictyostelium myosin II. *Biochemistry* 2002;41:9525–9534. [PubMed: 12135375]
29. Philo JS. A method for directly fitting the time derivative of sedimentation velocity data and an alternative algorithm for calculating sedimentation coefficient distribution functions. *Anal. Biochem* 2000;279:151–163. [PubMed: 10706784]
30. Trybus KM. Filamentous smooth muscle myosin is regulated by phosphorylation. *J. Cell Biol* 1989;109(6 Pt 1):2887–2894. [PubMed: 2531749]
31. Sheng S, Gao Y, Khromov AS, Somlyo AV, Somlyo AP, Shao Z. Cryo-atomic force microscopy of unphosphorylated and thiophosphorylated single smooth muscle myosin molecules. *J. Biol. Chem* 2003;278:39892–39896. [PubMed: 12907680]
32. Woodhead JL, Zhao FQ, Craig R, Egelman EH, Alamo L, Padron R. Atomic model of a myosin filament in the relaxed state. *Nature* 2005;436:1195–1199. [PubMed: 16121187]
33. Wendt T, Taylor D, Messier T, Trybus KM, Taylor KA. Visualization of head-head interactions in the inhibited state of smooth muscle myosin. *J. Cell Biol* 1999;147:1385–1390. [PubMed: 10613897]
34. Sellers JR, Eisenberg E, Adelstein RS. The binding of smooth muscle heavy meromyosin to actin in the presence of ATP. Effect of phosphorylation. *J. Biol. Chem* 1982;257(23):13880–13883. [PubMed: 6128340]
35. Rovner AS, Freyzo Y, Trybus KM. Chimeric substitutions of the actin-binding loop activate dephosphorylated but not phosphorylated smooth muscle heavy meromyosin. *J. Biol. Chem* 1995;270:30260–30263. [PubMed: 8530442]
36. Sherwood JJ, Waller GS, Warshaw DM, Lowey S. A point mutation in the regulatory light chain reduces the step size of skeletal muscle myosin. *Proc. Natl. Acad. Sci. U. S. A* 2004;101:10973–10978. [PubMed: 15256600]
37. Tyska MJ, Dupuis DE, Guilford WH, Patlak JB, Waller GS, Trybus KM, Warshaw DM, Lowey S. Two heads of myosin are better than one for generating force and motion. *Proc. Natl. Acad. Sci. U. S. A* 1999;96:4402–4407. [PubMed: 10200274]
38. Kad NM, Rovner AS, Fagnant PM, Joel PB, Kennedy GG, Patlak JB, Warshaw DM, Trybus KM. A mutant heterodimeric myosin with one inactive head generates maximal displacement. *J. Cell Biol* 2003;162:481–488. [PubMed: 12900396]
39. Harris DE, Warshaw DM. Smooth and skeletal muscle myosin both exhibit low duty cycles at zero load *in vitro*. *J. Biol. Chem* 1993;268:14764–14768. [PubMed: 8325853]
40. Trybus KM. No strain, no gain. *Nat. Cell Biol* 2005;7:854–856. [PubMed: 16136183]
41. Murphy, RA.; Gerthoffer, WT. Cell calcium and contractile system regulation in arterial smooth muscle. In: Opie, LH., editor. *Calcium Antagonists and Cardiovascular Disease*. Raven Press; New York: 1984. p. 75–84.
42. Murphy RA. What is special about smooth muscle? The significance of covalent crossbridge regulation. *Faseb J* 1994;8:311–318. [PubMed: 8143937]
43. Hai CM, Murphy RA. Cross-bridge phosphorylation and regulation of latch state in smooth muscle. *Am. J. Physiol* 1988;254:C99–C106. [PubMed: 3337223]
44. Khromov AS, Webb MR, Ferenczi MA, Trentham DR, Somlyo AP, Somlyo AV. Myosin regulatory light chain phosphorylation and strain modulate adenosine diphosphate release from smooth muscle Myosin. *Biophys. J* 2004;86:2318–2328. [PubMed: 15041670]

45. Khromov A, Somlyo AV, Somlyo AP. MgADP promotes a catch-like state developed through force-calcium hysteresis in tonic smooth muscle. *Biophys. J* 1998;75:1926–1934. [PubMed: 9746533]
46. Vyas TB, Mooers SU, Narayan SR, Witherell JC, Siegman MJ, Butler TM. Cooperative activation of myosin by light chain phosphorylation in permeabilized smooth muscle. *Am. J. Physiol* 1992;263:C210–C219. [PubMed: 1386187]

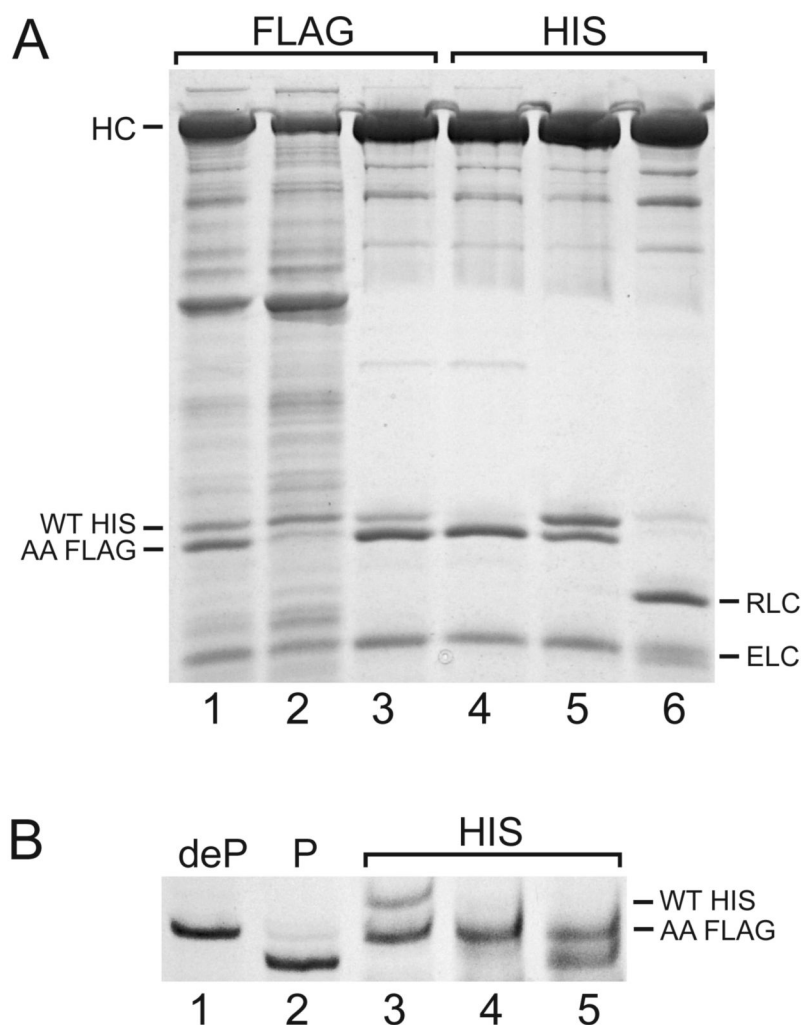


Figure 1.

Purification of 1-P HMM. A. 12% polyacrylamide SDS gel. Lanes 1-3 are from the FLAG column: (1) load, (2) flow-through, (3) elution. Lanes 4-6 are from the nickel chelate column: (4) non-specifically bound protein displaced with 15 mM imidazole buffer, (5) elution of 1-P HMM, (6) 1-P HMM after removal of epitope tags with thrombin. B. Charge gel of dissociated RLCs. Lanes 1-2 are dephosphorylated (deP) and phosphorylated (P) RLC standards. Lanes 3-5: purified 1-P HMM (3) before, and (4) after removal of epitope tags, and (5) after phosphorylation. The positions of the tagged RLCs are indicated by horizontal lines.

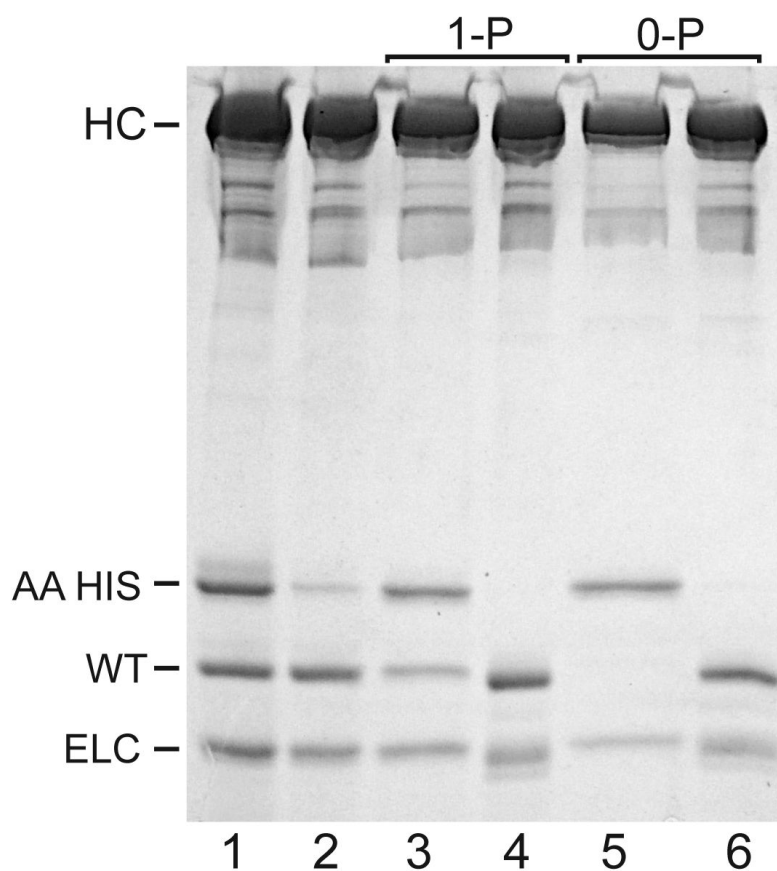


Figure 2.

Purification of 1-P myosin on the nickel chelate column. Lane (1) load, (2) non-specifically bound protein displaced with 15 mM imidazole buffer, (3) 1-P myosin eluted between 30 and 60 mM Imidazole, (4) 1-P myosin after thrombin cleavage, (5) doubly exchanged 0-P myosin eluted between 95 and 125 mM imidazole, (6) 0-P myosin after thrombin cleavage. 12% polyacrylamide SDS gel.

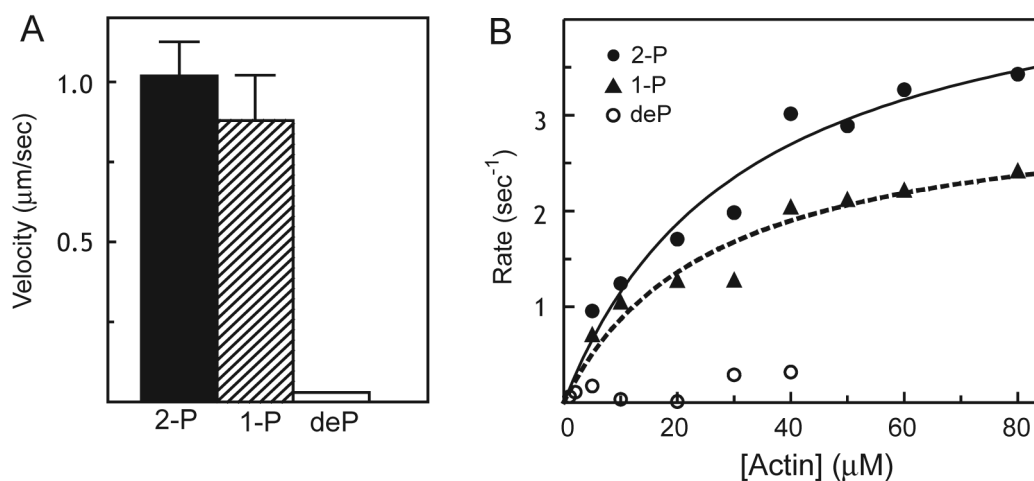


Figure 3.

Motility and steady-state ATPases of HMM species. A. In vitro actin filament velocity \pm standard deviation. 2-P HMM (110 filaments from two independent preparations) and 1-P HMM (207 filaments from 4 preparations) were assessed. deP HMM was analyzed but did not move actin. B. Average steady-state actin-activated ATPase activity of 2-P HMM (filled circles), deP HMM (open circles), 1-P HMM (filled triangles) from two independent assays. The V_{\max} values were $3.1 \pm 0.4 \text{ sec}^{-1}$ (1-P HMM) and $4.8 \pm 0.6 \text{ sec}^{-1}$ (2-P HMM). K_M s were $26 \pm 9 \text{ } \mu\text{M}$ (1-P HMM) and $32 \pm 10 \text{ } \mu\text{M}$ (2-P HMM). An independent preparation confirmed 1-P HMM had $\sim 75\%$ the V_{\max} value of 2-P HMM.

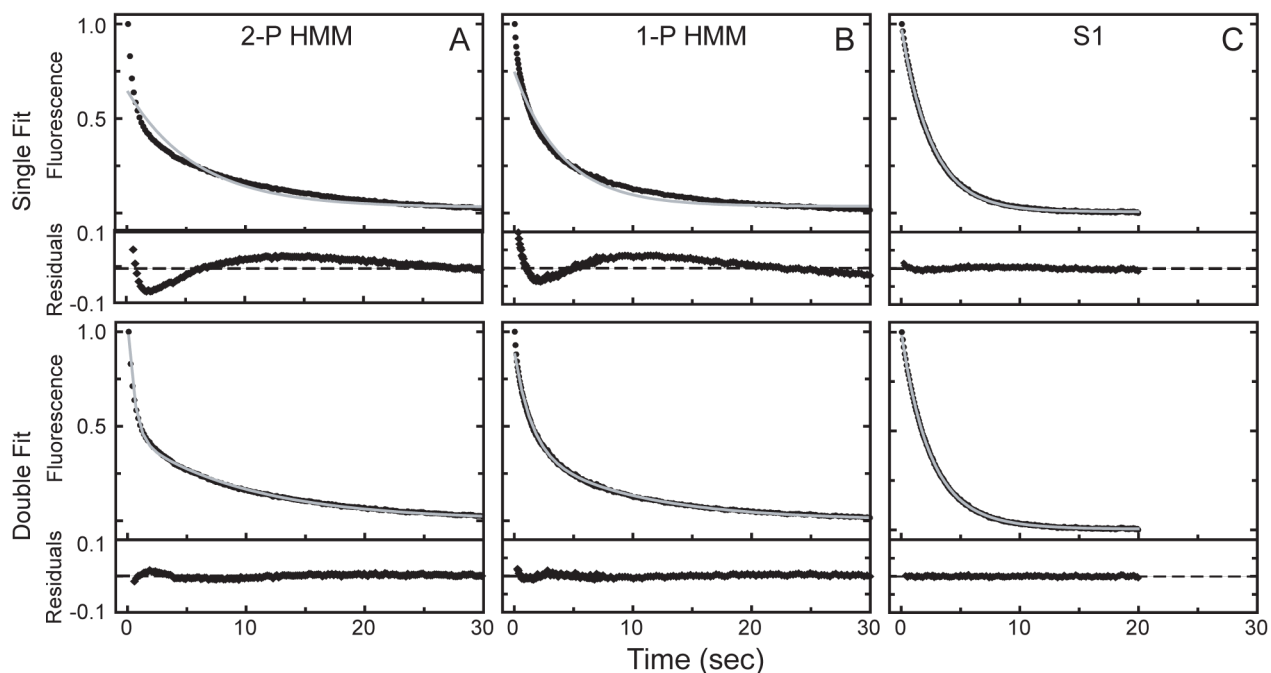


Figure 4.

Single ATP turnovers by HMM species and S1 in the presence of actin. The decrease in mant-ATP fluorescence was plotted as a function of time and fitted by single (upper panel) and double (lower panel) exponential equations (gray lines). Residuals are graphed below. Derived single and double exponential rate constants (with proportion of total signal amplitude in parentheses) \pm SD of the fit are listed for the following species. A. 2-P HMM. Single rate $0.172 \pm .006 \text{ sec}^{-1}$, double rates $1.78 \pm .034 \text{ sec}^{-1}$ (57%) and $0.10 \pm .001 \text{ sec}^{-1}$ (43%) B. 1-P HMM. Single rate $0.276 \pm .006 \text{ sec}^{-1}$, double rates $0.91 \pm .021 \text{ sec}^{-1}$ (53%) and $0.127 \pm .003 \text{ sec}^{-1}$ (47%). C. S1. Single rate $0.392 \pm .001 \text{ sec}^{-1}$, double rates $0.63 \pm .044 \text{ sec}^{-1}$ (30%) and $0.33 \pm .009 \text{ sec}^{-1}$ (70%). Amplitudes were normalized to the full-scale signal. Conditions: 10 mM NaCl, 10 mM imidazole-HCl (pH 7.0), 1 mM EGTA, 1 mM MgCl_2 , 1 mM DTT, temperature 30°C , $0.5 \mu\text{M}$ HMM, $1 \mu\text{M}$ mant-dATP, 3 mM MgATP, $10 \mu\text{M}$ actin.

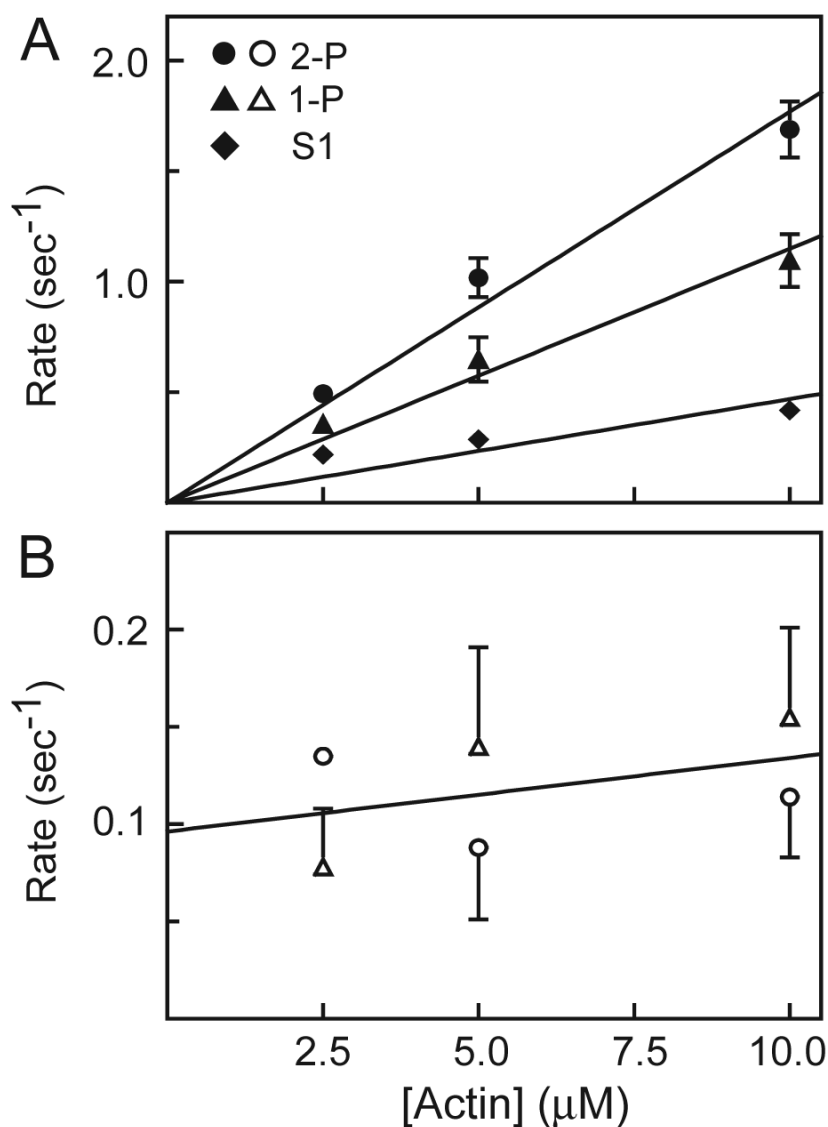


Figure 5.

Mant-dATP single turnover rates for the 3 HMM species and S1 as a function of actin. A. Fast rates \pm SD for 2-P HMM (filled circles), 1-P HMM (filled triangles), and S1 (filled diamonds). Lines are best-fit linear regressions. B. Slow rates \pm standard deviation for 2-P HMM (open circles), and 1-P HMM (open triangles). Line is best fit for combination of 1-P and 2-P data. HMM data are from 3-5 protein preparations, except the 2.5 μ M point for 2-P HMM (2 preparations). S1 data from 3 assays, except 2.5 μ M point is the average of two determinations. Each preparation was assayed 1-4 times, with each assay reporting the best fit to the average of three independent mixing experiments. Error bars for S1 and the 2.5 μ M data point for 2-P are smaller than the symbol.

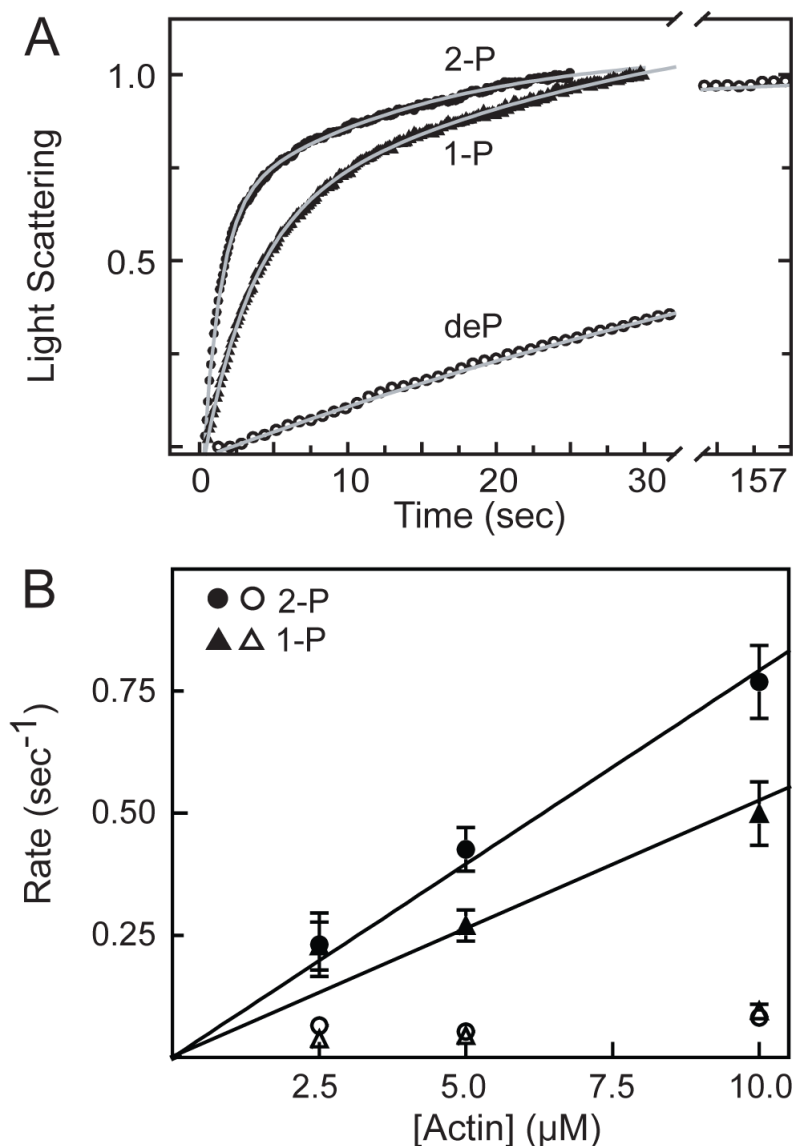
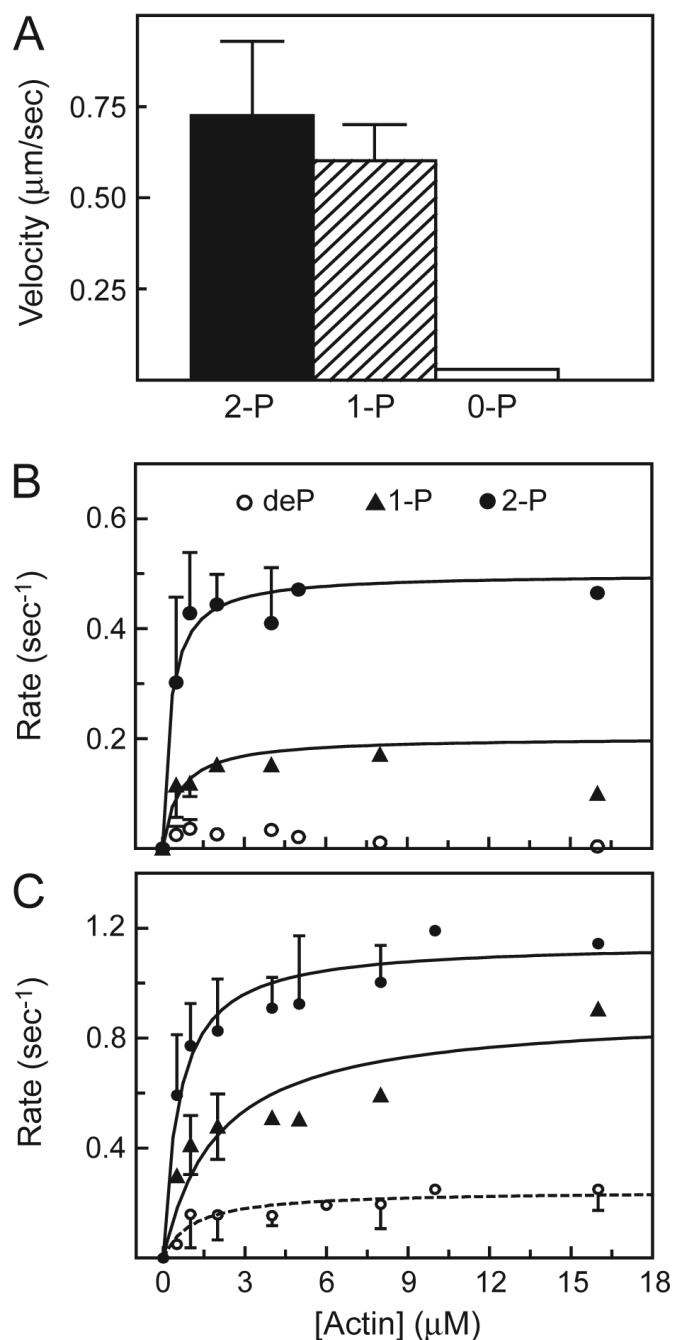


Figure 6.

HMM single ATP turnovers by light scattering. A. Raw data time courses for 2-P (filled circles), 1-P (filled triangles), and deP HMMs (open circles) with fitted exponential equations (gray lines). The double exponential rate constants \pm the standard deviation of the fit (with proportion of total signal amplitude in parentheses) for 2-P HMM were $0.87 \pm .012 \text{ sec}^{-1}$ (65%) and $0.073 \pm .002 \text{ sec}^{-1}$ (35%), while rates for 1-P were $0.58 \pm .014 \text{ sec}^{-1}$ (53%) and $.044 \pm .002 \text{ sec}^{-1}$ (47%). The single rate for deP HMM was $0.013 \pm .0001 \text{ sec}^{-1}$. B. Single turnover rates for the 2-P (filled and open circles) and 1-P HMMs (filled and open triangles) plotted as a function of actin. Lines are best-fit linear regressions. Average \pm SD for 3-5 different protein preparations. Each preparation was assayed 1-4 times, with each assay reporting the best fit to the average of three independent mixing experiments. Error bars for the slower data are smaller than the symbol. Conditions: 10 mM NaCl, 10 mM imidazole-HCl (pH 7.0), 1 mM EGTA, 1 mM MgCl₂, 1 mM DTT, temperature 30°C, 0.5 μM HMM, 10 μM actin.

**Figure 7.**

Motility and steady-state ATPases of myosin species. A. In vitro actin filament velocity of 2-P (115 filaments; 3 preparations), 1-P (117 filaments; 2 preparations), and 0-P myosins (85 filaments; 2 preparations), following exchange and affinity chromatography. Bars denote average \pm SD. B. Actin-activated ATPase activity in the presence of 1 mM MgCl_2 . Data from deP (open circles), 1-P (filled triangles), and 2-P myosin (filled circles) were fit to the Michaelis-Menten equation. The V_{max} and K_M values were $0.50 \pm 0.02 \text{ sec}^{-1}$ and $0.3 \pm 0.1 \mu\text{M}$ for 2-P myosin, and $0.20 \pm 0.02 \text{ sec}^{-1}$ and $0.6 \pm 0.2 \mu\text{M}$ for 1-P myosin. C. Actin-activated ATPase activity in the presence of 10 mM MgCl_2 . The V_{max} and K_M values were $1.15 \pm 0.04 \text{ sec}^{-1}$ and $0.6 \pm 0.1 \mu\text{M}$ for 2-P myosin, $0.89 \pm 0.10 \text{ sec}^{-1}$ and $2.0 \pm 0.9 \mu\text{M}$ for 1-P myosin, and

$0.25 \pm 0.02 \text{ sec}^{-1}$ and $1.2 \pm 0.5 \text{ }\mu\text{M}$ for deP myosin. Points with error bars are the mean of >3 preparations \pm SD. Points without bars are the average of two preparations. The buffer for both B and C also contained 60 mM KCl, 10 mM imidazole-HCl, pH 7.0, 1 mM EGTA; 1 mM NaN_3 ; 1 mM DTT at 37° C.

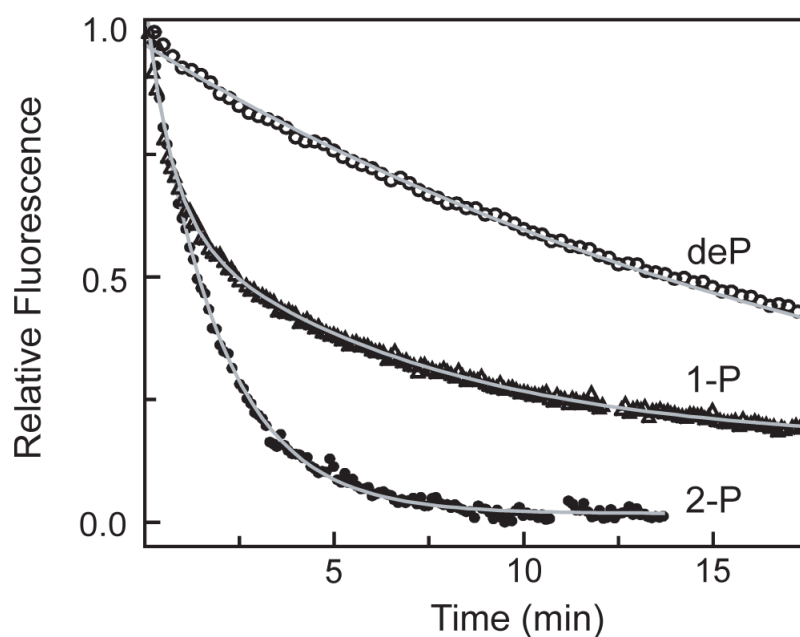


Figure 8.

Myosin single turnovers in the absence of actin. Fluorescence data time courses for 2-P myosin (filled circles), 1-P myosin (filled triangles), and deP myosin (open circles). Amplitudes were normalized to the full-scale fluorescence signal. Rate constants from single exponential fits to the data for deP ($0.08 \times 10^{-2} \text{ sec}^{-1}$) and 2-P myosin ($0.9 \times 10^{-2} \text{ sec}^{-1}$). 1-P myosin was better fit by a double exponential equation, giving rates of $2.5 \times 10^{-2} \text{ sec}^{-1}$ and $0.24 \times 10^{-2} \text{ sec}^{-1}$. A second experiment performed on each of these species gave rates within 15% of those shown here. Conditions: 100 mM NaCl, 10 mM imidazole-HCl (pH 7.0), 1 mM EGTA, 5 mM MgCl_2 , 1 mM DTT, temperature 30°C , $0.5 \mu\text{M}$ myosin, $1 \mu\text{M}$ mant-dATP.

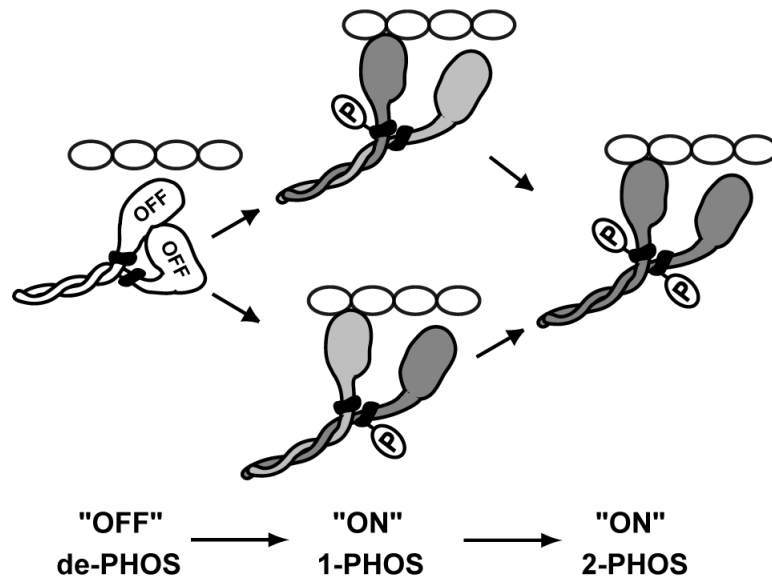


Figure 9.

Structural model for activation of 1-P smooth muscle HMM, based on data from dephosphorylated and phosphorylated HMM and myosin (11,12). Phosphorylation of a single RLC (black ring on neck) disrupts the asymmetric structure, freeing both heads (1-PHOS), and yielding a structure similar to 2-PHOS. The two versions of 1-PHOS indicate that the phosphorylated and dephosphorylated heads are almost equally likely to bind to actin. Shading indicates the extent of possible activation of the head, relative to the actin-activated head in doubly-phosphorylated myosin. The essential light chains are omitted for clarity.